Hemoglobin alpha regulates T-lymphocyte activation and mitochondrial function

Emily C. Reed[1,2], Tatlock H. Lauten[1,2], Tamara Natour[1,2], Lauren J. Pitts[1,2], Caroline N. Jojo[1,2], Brooke L. Griffin[1,2], Sreeram Pasupuleti[1,2], Adam J. Case[1,2*].

Affiliations:
[1]Department of Psychiatry and Behavioral Sciences, Texas A&M University, Bryan, TX, United States
[2]Department of Medical Physiology, Texas A&M University, Bryan, TX, 77807, United States

***Corresponding author:**
Adam J. Case, PhD
Associate Professor
Department of Psychiatry and Behavioral Sciences
Department of Medical Physiology
8447 John Sharp Pkwy
MREB2 3414
Bryan, TX 77807
Phone (979) 436-9709
Fax (979) 436-0062
Email: acase@tamu.edu

Conflict of Interest Statement: The authors have declared that no conflict of interest exists.

Abstract Word Count: 250
Total Word Count: 6,785
References: 50
Tables: 0
Figures: 4
Supplementary Figures: 4

Keywords: Hemoglobinopathy, immune, inflammation, redox, EAE

Abstract

Hemoglobinopathies affect approximately 7% of the global population and are associated with an increased risk of autoimmune disorders, though the underlying mechanisms remain unclear. Hemoglobin is traditionally recognized for its role in oxygen transport within erythrocytes, but its expression in other cell types has been documented. We have recently discovered hemoglobin alpha a1 (Hbα-a1 mRNA and Hbα protein) in T-lymphocytes and previously reported that its expression was sensitive to mitochondrial redox perturbations. However, outside of its incidence and basic characterization, the functional role of Hbα in T-lymphocytes remained unknown. Herein, we identify Hbα in both $CD4^+$ and $CD8^+$ T-lymphocyte subsets, and found its expression is highly dynamic, differs between the two subtypes, and is dependent upon activation stage. Further, the loss of Hbα impairs mitochondrial function, dysregulates cytokine production, and lowers the activation threshold primarily in $CD4^+$ T-lymphocytes, indicating a critical role for Hbα within this subset. While these data suggested the loss of Hbα in T-lymphocytes may promote aberrant activation of autoreactive T-lymphocytes, surprisingly, we discovered that mice lacking Hbα in T-lymphocytes exhibited reduced severity of experimental autoimmune encephalomyelitis (EAE) compared to wild-type control animals. Interestingly, T-lymphocytes lacking Hbα *in vivo* appeared to function identically to wild-type controls, which did not explain the protection against EAE. In contrast, T-lymphocyte Hbα knock-out mice displayed significantly reduced levels of circulating immunoglobulins and CD40L expression compared to their wild-type counterparts during EAE, suggesting impaired intercellular communication. These data elucidate a previously unrecognized role for Hbα in T-lymphocyte function with implications for hemoglobinopathies.

54 **Significance statement**

55 Hemoglobinopathies are diseases that affect hemoglobin. These diseases come with an increased risk
56 of developing autoimmune disorders, but it is unclear why this occurs. While classically thought to be confined
57 to red blood cells, hemoglobin has been identified in a variety of cell types. We recently discovered hemoglobin
58 inside T-lymphocytes, but its function inside these cells remained elusive. In this work, we identify that
59 hemoglobin in T-lymphocytes is essential to maintain mitochondrial metabolism, inflammatory protein
60 production, and communication with other immune cells. Together, our findings uncover that hemoglobin, a
61 protein not even known to exist in adaptive immune cells, is vital for T-lymphocyte function, and may explain
62 why patients with hemoglobinopathies have an increased risk of developing autoimmune disorders.

63 **Introduction**

64 Hemoglobinopathies are a class of genetic diseases in which one or more subunits of hemoglobin are
65 impacted, and are one of the world's most prominent inherited genetic disorders affecting around 7% of the
66 human population (1). The consequences of hemoglobinopathies are primarily attributed to decreased oxygen
67 (O_2) delivery by erythrocytes, but this explanation appears incomplete given the pathology associated with
68 these diseases. For example, hemoglobinopathies are elevate the risk of developing comorbid autoimmune
69 disorders, such as rheumatoid arthritis and systemic lupus erythematosus (2-4). These autoimmune disorders
70 are characterized by aberrant autoreactive immune cells, primarily of the adaptive immune system, but it is
71 unclear how mutations or alterations in hemoglobin would impact the development of these diseases. In fact,
72 low O_2 has been shown to decrease T-lymphocyte responses (5), which would suggest hemoglobinopathies
73 would be more likely to suppress the prevalence of comorbid autoimmune diseases. Therefore, we posited that
74 the impact of hemoglobin mutations solely in erythrocytes could not sufficiently explain the elevated risk of
75 autoimmunity in hemoglobinopathies.

76 Over the past 30 years, research has challenged the dogma that hemoglobin is strictly confined to
77 erythrocytes by identifying hemoglobin subunits expressed in a variety of other cell types, such as neurons (6-
78 8), macrophages (9), mesangial cells (10), and others (11, 12). Through these studies, hemoglobin has been
79 revealed to possess diverse redox abilities, including facilitating O_2 or nitric oxide (NO) exchange, modulating
80 iron utilization, antioxidant capabilities, protection during hypoxia, and mediating mitochondrial bioenergetics.
81 In a preliminary report, we discovered hemoglobin alpha-a1 (Hbα-a1 mRNA and Hbα protein) expression in
82 both mouse and human T-lymphocytes, showed its differential levels in various T-lymphocyte polarized states,
83 and elucidated its increased production in response to redox perturbations, indicating a potential antioxidant
84 function in these cells (13). We further demonstrated that Hbα overexpression led to an increase in
85 mitochondrial membrane potential, suggesting that Hbα in T-lymphocytes may also play a role in mitochondrial
86 homeostasis. Last, initial studies using T-lymphocyte-specific Hbα-a1 knock out mice (HbKO) depicted a
87 significant decrease in the percentage of naïve $CD4^+$ T-lymphocytes after psychological trauma, proposing
88 irregular cellular activation in the absence of Hbα-a1. Altogether, these data suggest that Hbα may be
89 necessary to prevent aberrant activation of T-lymphocytes by modulating the mitochondrial redox environment
90 within these cells.

91 Given these interesting preliminary results demonstrating a functional role for hemoglobin in T-
92 lymphocytes, we set out to explore if this protein was important in the regulation of autoimmunity. Herein, we
93 identify unique temporal Hbα-a1 mRNA and Hbα protein expression patterns in both $CD4^+$ and $CD8^+$ T-
94 lymphocytes, with the loss of Hbα in T-lymphocytes exhibiting a decrease in mitochondrial metabolism,
95 increase in proinflammatory cytokine production after 24-hour activation, and a decreased threshold for
96 activation compared to wild-type (WT) T-lymphocytes. Incongruously, HbKO animals showed better disease
97 outcomes in a preclinical model of autoimmune multiple sclerosis, known as experimental autoimmune
98 encephalomyelitis (EAE), despite virtually identical T-lymphocyte inflammatory phenotypes in HbKO and WT
99 animals. However, we uncover that this unexpected result may be due to impaired T-lymphocyte interactions
100 with other immune cells, such as B-lymphocytes, hindering EAE disease development. Together, this work
101 uncovers a vital functional role for Hbα in T-lymphocytes that suggests patients with hemoglobinopathies may
102 indeed possess direct immune alterations due to the loss or mutation of hemoglobin.

103 **Materials and Methods**

104 **Mice**

105 Wild-type C57BL/6J (#000664; shorthand WT) and B6.Cg-Tg(Cd4-cre)1Cwi/BfluJ (#022071; shorthand CD4-
106 cre) mice were obtained from Jackson Laboratories (Bar Harbor, ME, USA). Conditional Hbα-a1 knock-out
107 mice were graciously provided by Dr. Brant Isakson as previously described (14). CD4-cre is activated during
108 the double positive developmental stage in the thymus leading to cre recombination in both mature $CD4^+$ and
109 $CD8^+$ T-lymphocytes (15), therefore, conditional Hbα-a1 knock-out mice were crossed with CD4-Cre mice to
110 generate pan-T-lymphocyte-specific modified progeny (HbKO). All mice were bred in house to eliminate
111 shipping stress and microbiome shifts, as well as co-housed with their littermates (≤5 mice per cage) prior to
112 the start of experimentation to eliminate social isolation stress. Mice were housed with standard pine chip
113 bedding, paper nesting material, and given access to standard chow (#8604 Teklad rodent diet, Inotiv, West
114 Lafayette, IN, USA) and water ad libitum. Male and female experimental mice between the ages of 8-14 weeks
115 were utilized in all experiments. If no significant sex differences were observed, data are presented as pooled
116 independent of sex to increase N while reducing unnecessary animal use (16). Experimental mice were
117 randomized, and when possible, experimenters were blinded to the respective cohorts until the completion of
118 the study. Mice were sacrificed by pentobarbital overdose (150 mg/kg, Fatal Plus, Vortech Pharmaceuticals,
119 Dearborn, MI, USA) administered intraperitoneally. All mice were sacrificed between 7:00 and 9:00 Central
120 Time to eliminate circadian rhythm effects on T-lymphocyte function. All procedures were reviewed and
121 approved by Texas A&M University Institutional Animal Care and Use Committees.

122

123 **Mouse T-lymphocyte isolation, culture, and activation**

124 Primary immune cells were collected from mice as previously described (13). Briefly, spleens or inguinal lymph
125 nodes were collected and disrupted into a single cell suspension then passed through a 70 μM nylon mesh
126 filter (#22363548, ThermoFisher Scientific). Erythrocytes were removed using red blood cell lysis buffer (150
127 mM NH_4Cl, 10 mM $KHCO_3$, 0.1 mM EDTA). Splenic T-lymphocytes were negatively selected using EasySep
128 Mouse total, $CD4^+$, or $CD8^+$ T-cell negative magnetic isolation kit (StemCell Technologies #19851, #19852,
129 #19853), per manufacturer's instructions. T-lymphocytes were counted, and viability was assessed using
130 Trypan Blue exclusion on a Bio-Rad TC20 Automated Cell Counter. For activation, cells were plated at 800,000

131 cells/mL with anti-CD3/28 Dynabeads (Dynabeads, #11456D) in a 1:1 cell to bead ratio in T-lymphocyte media
132 consisting of RPMI media supplemented with 10% Fetal Bovine Serum, 2 mM Glutamax, 10 mM HEPES, 100
133 U/mL penicillin/streptomycin, and 50 μM of 2-mercaptoethanol. Cells were cultured in 5% CO_2, 37°C incubator
134 (HERAcell Vios 160i CO_2 incubator, ThermoFisher Scientific).
135

136 **Experimental autoimmune encephalomyelitis (EAE) and restimulation**

137 *Disease induction*

138 EAE was induced using the MOG_{35-55}/CFA Emulsion kit (#EK-2110, Hooke Laboratories) as described in (17).
139 Briefly, 9-14 week old mice were anesthetized and injected with 100 μl of myelin oligodendrocyte glycoprotein
140 (MOG) emulsion in two separate subcutaneous locations. Two hours later, mice were anesthetized again and
141 injected intraperitoneally with 100 μL of 100 ng/μL pertussis toxin in PBS, followed by a second dose after 24
142 hours. Beginning seven days later, mice were weighed and scored every day to assess disease progression.
143 Disease scores (0-5) were based off a standardized clinical signs and symptom rubric, described in detail in
144 (17). Separate cohorts of mice were sacrificed at either peak disease (day 14) or after disease relapse (day
145 28).

146 *Restimulation*

147 Total immune cells were isolated from spleens or inguinal lymph nodes as described above and cultured for 72
148 hours in the presence of 10 μg/mL of MOG_{35-55} (#NC0754019, Hooke Laboratories). Cells counts were
149 assessed, and media was analyzed for extracellular proinflammatory cytokine production.
150

151 **Flow cytometry immunophenotyping and redox assessment**

152 T-lymphocytes were immunophenotyped via 4-laser Attune NxT flow cytometer (ThermoFisher Scientific) as
153 previously described (18). Cells were stained with 1:1000 dilutions of CD3ε PE-Cy7 (#25-0031-82,
154 ThermoFisher Scientific), CD4 eFluor 506 (#69004182, ThermoFisher Scientific), CD8 Super Bright 702
155 (#67008182, ThermoFisher Scientific), CD19 APC-Cy7 (#BDB557655, Thermo Fisher Scientific), CD11b
156 BV421 (#BDB562605, Thermo Fisher Scientific), CD11c APC, (#501129650, Thermo Fisher Scientific)
157 antibodies along with 1 μM MitoSOX Red (#M36008, ThermoFisher Scientific) in RPMI media to assess
158 mitochondrial reactive oxygen species (ROS) in various immune cell subpopulations. Mean fluorescence

159 intensity (MFI) of MitoSOX Red was reported as a readout of mitochondrial ROS levels. Cells were stained
160 with 100 nM tetramethylrhodamine ethyl ester (TMRE) (#T669, ThermoFisher Scientific) to measure
161 mitochondrial membrane potential. Antibodies for staining other extracellular T-lymphocyte markers include
162 CD28 APC (5014933, Thermo Fisher Scientific), CD27 Super Bright™ 600 (63027182, Thermo Fisher
163 Scientific), and CD40L Alexa Fluor™ 488 (53154182, Thermo Fisher Scientific). Additionally, T-lymphocytes
164 were also assessed for various polarization states, as previously described in (19, 20). Briefly, splenic or
165 inguinal lymph node immune cells were treated with phorbol 12-myristate-13-acetate (10 ng/mL)
166 (#5005820001, Thermo Fisher Scientific), BD GolgiPlug (#BDB555029, Thermo Fisher Scientific) and
167 ionomycin (0.5 mg/mL) (#AAJ60628LB0, Thermo Fisher Scientific) for 4 hours at 37°C. Cells were then stained
168 with Live-Dead Fixable Far Red viability dye (#501121530, Thermo Fisher Scientific) for 30 minutes, 4°C,
169 washed, then followed by a 1:1000 dilution of extracellular antibodies for CD3ε PE-Cy7 (#25-0031-82, Thermo
170 Fisher Scientific), CD4 eFluor 506 (#69004182, Thermo Fisher Scientific), and CD8 Alexa Fluor™ 488 (#69-
171 0041-82, Thermo Fisher Scientific) for 30 minutes at 4°C. Afterwards, cells were fixed and permeabilized with
172 FOXP3/Transcription Factor Staining Buffer Set according to manufacturer's instructions (#501128857,
173 Thermo Fisher Scientific). Cells were stained with 1:1000 dilutions of intracellular antibodies against IFNγ APC-
174 eFluor780 (#47-7311-82, Thermo Fisher Scientific), IL-4 BV421 (#562915, BD Biosciences), FoxP3 PE-
175 Cyanine5.5 (#35-5773-82, Thermo Fisher Scientific), and IL-17 BV711 (#407-7177-82, Thermo Fisher
176 Scientific). All flow cytometry data was analyzed using FlowJo v10 software (BD Biosciences).
177

178 **RNA extraction, cDNA production, and quantitative real-time RT-PCR**

179 T-lymphocyte RNA isolation and mRNA levels were assessed as previously described (13, 21). Briefly, mRNA
180 was extracted using the RNAeasy plus mini kit (#74136, Qiagen) and quantified using NanoDrop One
181 Spectrophotometer (#13400518, Thermo Scientific). RNA was then transformed into cDNA using
182 ThermoFisher High-Capacity cDNA Reverse Transcriptase Kit (#4374967, Applied BioSystem). Generated
183 cDNA was used for real time quantitative PCR. Primers for genes of interest were designed using NIH primer-
184 BLAST spanning exon-exon junctions. Cq values were determined, and relative gene expression was
185 calculated by comparing housekeeping 18s ribosomal gene expression to gene of interest (2^{-ddCq}).
186

187 **Protein analysis**

188 Protein was isolated from T-lymphocytes using RIPA lysis buffer (#PI89900, Thermo Scientific) and 1% Halt
189 protease inhibitor cocktail (#PI87785, Thermo Scientific). Samples were subsequently subjected to sonication
190 and centrifugation to obtain soluble protein, which was quantified using Pierce BCA protein assay kit
191 (#PI23227, Thermo Scientific). Hbα protein was assessed via Total Protein Jess Automated Western Blot (Bio-
192 techne) as described in (13, 21) using anti-Hbα primary antibody - Rabbit (#PIPA579347, Fisher) 1:20. Analysis
193 was performed using Compass Software for Simple Western v6.1.0.

194

195 **Seahorse Mitochondrial Stress Test**

196 T-lymphocyte mitochondrial metabolism assessment was performed as previously described (13, 21). Briefly,
197 activated T-lymphocytes were plated in Seahorse XF RPMI media (#103576-100, Agilent) supplemented with
198 10 mM Seahorse XF Glucose (#103577-100, Agilent), 1 mM Seahorse XF Pyruvate (#103578-100, Agilent), 2
199 mM Seahorse XF L-Glutamine (#103579-100, Agilent). Cells were adhered to seahorse cell microplates using
200 1 μg/cm^2 Cell-Tak (#354240, Corning) and seeded at a density of 200,000 cells per well. Mitochondrial
201 inhibitors (1 μM Oligomycin, 1 μM 4-trifluoromethoxy-phenylhydrazone (FCCP), 0.5 μM Rotenone and
202 Antimycin, #103015-100, Agilent), were injected into each well and oxygen consumption rate (OCR) was
203 measured via Seahorse XFe96 Analyzer.

204

205 **Single-cell energetic metabolism by profiling translation inhibition (SCENITH)**

206 Protein translation inhibition was measured as a proxy for ATP production, as described in detail in (22). Naïve
207 or 72-hour activated splenic T-lymphocytes were plated (in duplicate per treatment group) at 500,000 cells per
208 well in a 96 well plate. Cells were treated with 100 mM of 2-deoxy-D-glucose (2-DG), 1μM oligomycin
209 (#103020-100, Agilent), or both for 45 minutes at 37°C. During the last 15 minutes of incubation, 10 μg/mL of
210 puromycin (#A1113803, Thermo Fisher Scientific) was added to each well. Cells were washed, stained with
211 Fixable Viability dye eFluor (#501128817, Thermo Fisher Scientific) for 30 minutes at 4°C, then subsequently
212 stained with 1:1000 CD4 eFluor 506 (#69004182, ThermoFisher Scientific) and CD8 Alexa Fluor™ 488 (#69-
213 0041-82, Thermo Fisher Scientific) extracellular antibodies. Cells were fixed and permeabilized (#501128857,
214 Thermo Fisher Scientific), then intracellularly stained with 1:1000 anti-puromycin Alexa Fluor™ 647 antibody

215 (#ab322729, Abcam) for 30 minutes at 4°C. Cells were then resuspended in PBS and fluorescence was
216 detected using the 4-laser Attune NxT flow cytometer (ThermoFisher Scientific). MFI of puromycin in live $CD4^+$
217 and $CD8^+$ T-lymphocytes was calculated using FlowJo v10 software (BD Biosciences). Average MFI of each
218 experimental group for each sample was calculated, and mitochondrial dependence, glycolytic capacity,
219 glucose dependence, and fatty acid/amino acid oxidation capacity were determined as described in (22).
220

221 **Cytokine protein analysis**

222 Cytokine protein levels from *in-vivo* (i.e., plasma) and *ex-vivo* (i.e., media normalized to cell counts)
223 experiments were analyzed using Mesoscale multi-plex technology (Mesoscale Discovery), as described in
224 (19). Briefly, protein concentrations were assessed using custom Mesoscale Discovery U-Plex kits (Mesoscale
225 Discovery, Rockville, MD, USA) simultaneously targeting IL-1β, IL-2, IL-4, IL-6, IL-10, IL-17A, IFNγ, and TNFα
226 per manufacturer's instructions. Analysis was performed using a Mesoscale QuickPlex SQ 120 and analyzed
227 using Mesoscale Discovery software.
228

229 **Immunoglobulin ELISA**

230 Plasma immunoglobin concentration was determined using Invitrogen™ Mouse Ig Isotyping Instant ELISA™
231 Kit (#501125163, Thermo Fisher). Plasma was collected from EAE animals as described above and diluted
232 1:10 prior to analysis. Assay was performed according to manufacturer's instructions with analysis performed
233 at 450 nm using SpectraMax i3x multimode plate reader (Molecular Devices).
234

235 **Complete blood count (CBC)**

236 Blood parameters were assessed by complete blood count. Mice were sacrificed and blood was obtained via
237 cardiac puncture. Undiluted blood (25 µL) was then transferred into a microvette (#NC9141704, Fisher
238 Scientific) and analyzed by Abaxis VetScan HM5 Color Hematology System.
239

240 **Activation threshold**

241 T-lymphocyte activation threshold was assessed by isolating $CD4^+$ and $CD8^+$ T-lymphocytes as described
242 above, and plating with constant concentration of anti-CD28 (1 µg/mL) (#76556-222, VWR) and variable

243 concentration of anti-CD3 (0.01-10 µg/mL) (#76556-606, VWR) soluble antibodies. Media was harvested 24
244 hours later, and cytokine protein expression was assessed via Mesoscale.
245
246 **Migration assay**
247 T-lymphocyte migration was assessed using a transwell migration assay. Splenic $CD4^+$ and $CD8^+$ T-
248 lymphocytes were isolated and activated with Dynabeads for 72 hours. Cells were then counted and 1 x 10^6
249 cells were plated into the apical side of a 5 µM Millicell® 24 well hanging cell culture insert (#PTMP24H48,
250 Millipore Sigma) in FBS-free media. FBS-free media only (control) or media supplemented with 100 ng/mL
251 CXCL12 (#478-MR-025/CF, Biotechne) or 100 ng/mL RANTES (#460-SD-050/CF, Biotechne) was added on
252 the basolateral side of the insert. After 4 hours, basolateral side media was collected and migrated T-
253 lymphocyte counts were assessed by flow cytometry. Ratio of migrated cells was calculated by dividing
254 chemokine migrated cell count by control migrated cell count.
255
256 **Statistical analysis**
257 All data presented as mean ± standard error of the mean (SEM), with N values representing individual mice
258 listed in figure legends. Normality was assessed using Shapiro-Wilk normality test before statistical analysis.
259 For two group comparisons, Student's t-test was utilized. For experiments with 3 or more groups, an ordinary
260 one-way ANOVA was performed. Experiments containing two categorical groups were assessed using two-way
261 ANOVA or mixed-effects analysis. All statistics were completed using GraphPad Prism version 10.5.0.

262 **Results**

263 *Activation state of T-lymphocytes determines intracellular Hbα levels and impact on mitochondria*

264 While we reported the expression of Hbα-a1 in T-lymphocytes (13), the dynamics of its expression
265 during cellular activation remained unknown. To address this knowledge gap, splenic $CD4^+$ and $CD8^+$ T-
266 lymphocytes were isolated from WT mice, Hbα-a1 mRNA and Hbα protein levels were assessed 24-, 48- and
267 72-hours post-activation, and values normalized to the respective naïve cell-type levels. In contrast to
268 significant reductions in mRNA levels at 24 hours post-activation, Hbα protein content increased in both $CD4^+$
269 and $CD8^+$ T-lymphocytes compared to naïve T-lymphocytes (**Figure 1A-D**). Congruent with 48-hour mRNA
270 levels, Hbα protein decreased in both subtypes, but diverged between $CD4^+$ and $CD8^+$ at 72 hours (**Figure 1A-**
271 **D**). The highly variable expression of Hbα throughout the first 72 hours of T-lymphocyte activation highlights
272 the temporal and diverse regulation of Hbα within activated T-lymphocytes, and suggests differential
273 importance within T-lymphocyte subtypes.

274 To investigate the mechanistic function of Hbα-a1 in T-lymphocytes, we next generated a T-lymphocyte
275 specific Hbα-a1 knock out (HbKO) mouse model (**Supplementary Figure 1A**). Cre-mediated DNA
276 recombination was confirmed to be confined solely to T-lymphocytes (**Supplementary Figure 1B**), and T-
277 lymphocyte-specific loss of Hbα-a1 did not impact any erythrocyte or leukocyte parameter on complete blood
278 count analysis (**Supplementary Figure 1C-F**). Further, Hbα-a1 knock-out did not affect the percentage or cell
279 counts of either $CD4^+$ or $CD8^+$ splenic T-lymphocytes, suggesting loss of Hbα-a1 does not significantly impact
280 T-lymphocyte viability during development (**Supplementary Figure 1G-J**). *Ex-vivo* proliferative capacity was
281 also not hindered by the loss of Hbα-a1 in either T-lymphocyte subtype (**Supplementary Figure 1K-L**).

282 Given that we previously demonstrated that T-lymphocyte Hbα-a1 expression was highly sensitive to
283 redox perturbations primarily stemming from the mitochondria (13), we next sought to explore T-lymphocytes
284 mitochondrial bioenergetics in the absence of Hbα-a1. We observed a modest, but significant, increase in
285 mitochondrial reactive oxygen species (ROS) levels only in activated $CD4^+$ HbKO T-lymphocytes compared to
286 WT $CD4^+$ cells (**Figure 1E**), with no differences observed in activated $CD8^+$ or naïve cells of either subtype
287 (**Figure 1F, Supplemental Figure 1M-N**). Additionally, no significant differences were noted in either total
288 cellular ROS or NO levels in either $CD4^+$ and $CD8^+$ HbKO T-lymphocytes (**Supplemental Figure 1O-R**), which
289 suggested a primary impact of Hbα on the mitochondria. Indeed, mitochondrial membrane potential of both

290 $CD4^+$ and $CD8^+$ HbKO activated T-lymphocytes was significantly decreased compared to their WT counterparts
291 **(Figure 1G-H),** indicating the potential of mitochondrial metabolic perturbations. Indeed, $CD4^+$ HbKO T-
292 lymphocytes displayed significantly lower mitochondrial O_2 consumption, with the cells showing a significantly
293 lower maximum respiratory capacity compared to WT $CD4^+$ activated T-lymphocytes (**Figure 1I-J**). However,
294 while $CD8^+$ HbKO T-lymphocytes showed a slight decrease in O_2 consumption, these effects did not reach
295 statistical significance **(Figure 1K-L)**. Additionally, protein translation is known to be tightly coupled to ATP
296 production, and thus inhibition of ATP synthesis pathways (i.e., glycolysis and or mitochondrial oxidative
297 phosphorylation) can provide an indirect snapshot of metabolic dependencies (22). Interestingly, neither $CD4^+$
298 or $CD8^+$ activated HbKO T-lymphocytes showed any differences in mitochondrial dependence or glycolytic
299 capacity compared to WT T-lymphocytes **(Figures 1M-N, 1Q-R)**. However, there was a significant increase in
300 glucose dependence, coupled with a significant decrease in fatty acid/amino acid oxidation in HbKO T-
301 lymphocytes **(Figures 1O-P, 1S-T)**. Altogether, these data suggest Hbα-a1 plays a significant role in
302 maintaining mitochondrial function and redox balance in activated T-lymphocytes, particularly in $CD4^+$
303 subtypes.
304
305 *Activated HbKO T-lymphocytes exhibit an accelerated and enhanced proinflammatory phenotype*
306 We and others have previously demonstrated an important role for mitochondrial metabolism and redox
307 in shaping T-lymphocyte activation and effector functions (18, 23-26). Given the impact of Hbα on
308 mitochondrial redox and metabolic parameters, we hypothesized Hbα loss would significantly alter activation in
309 T-lymphocytes. Strikingly, $CD4^+$ HbKO T-lymphocytes produced higher levels of all cytokines post-activation
310 compared to WT T-lymphocytes, suggesting the Hbα knock-out leads to a loss of cytokine regulation post-
311 activation **(Figure 2A-D, Supplementary Figure 2A-D)**. In contrast, only IL-6 and IL-17A were impacted in
312 $CD8^+$ T-lymphocytes (**Figure 2E-H, Supplementary Figure 2E-H**), once again supporting a greater impact of
313 Hbα loss in $CD4^+$ T-lymphocytes. Furthermore, HbKO $CD4^+$ T-lymphocytes displayed higher levels of cytokines
314 throughout an increasing amount of CD3 stimulation, with HbKO $CD8^+$ T-lymphocytes showing minimal impact
315 (**Figure 2 I-P**), suggesting a lower threshold of activation specifically in $CD4^+$ cells. Overall, these data indicate
316 that the loss of HbKO in T-lymphocytes potentiates the magnitude and timing of activation-associated
317 cytokines, which primarily impacts $CD4^+$ subtypes.

318

319 *HbKO EAE animals exhibit better disease phenotypes but similar inflammatory profiles as WT EAE animals*

320 To assess the impact of Hbα loss on T-lymphocyte function *in vivo*, we induced a T-lymphocyte-
321 dependent model of experimental autoimmune encephalomyelitis (EAE) in WT and HbKO animals. Given the
322 observation of potentiated cytokine production in the absence of Hbα *ex vivo*, we hypothesized that HbKO
323 animals would have significantly worsened EAE disease progression. Contrary to our hypothesis, HbKO
324 animals had delayed disease progression, significantly lower EAE disease severity scores, and diminished
325 weight loss over the experimental period **(Figure 3B-C, Supplementary Figure 3B-C)**. Surprisingly, circulating
326 plasma cytokines levels were identical between WT and HbKO animals at both 14 and 28 days post
327 immunization (**Figure 3D-G, Supplementary Figure 3D-G).** Additionally, the only change in T-lymphocyte
328 population noted was a significantly decreased proportion of $CD4^+$ T-lymphocytes in draining lymph nodes at
329 28 days in HbKO animals (**Figure 3I**). In contrast, all other populations (including T_H1 and T_H17 cells, which are
330 highly causal in EAE disease progression (27)) at 14 and 28 days in both the spleen and lymph nodes showed
331 no differences compared to WT animals (**Figure 3H-O, Supplementary Figure 3H-O, 4A-D),** emphasizing that
332 loss of T-lymphocyte Hbα does not inhibit *in vivo* $CD4^+$ polarization and likely does not account for the
333 difference in EAE scores**.** Moreover, there was no significant difference in percentage of other splenic immune
334 cell populations, total immune cell infiltration into the spinal cord, or splenic T-lymphocyte mitochondrial ROS
335 between the two genotypes **(Supplementary Figure 4E-K)**. Last, T-lymphocyte memory also appeared
336 unimpacted by the loss of Hbα given that MOG_{35-55} antigen recall showed no differences in cellular proliferation
337 or cytokine production per cell at either 14 or 28 days post-EAE immunization in the spleen (**Figure 3P-S,**
338 **Supplementary Figure 3P-S, Supplementary Figure 4L**) or lymph nodes (data not shown).Together, these
339 puzzling findings show that HbKO mice possess a significantly decreased susceptibility to EAE compared to
340 WT mice, but the mechanism underlying this difference does not appear to be directly related to primary T-
341 lymphocyte effector functions.

342

343 *Loss of Hbα impairs T-lymphocyte intercellular communication*

344 Given the decreased percentage of $CD4^+$ T-lymphocytes in the draining lymph nodes of HbKO EAE
345 mice compared to WT mice (**Figure 3I**), we postulated that the loss of Hbα may alter the ability of T-

346 lymphocytes to appropriately migrate to chemotactic stimuli. However, neither $CD4^+$ or $CD8^+$ HbKO T-
347 lymphocytes demonstrated any deficiency in chemotactic migration *ex-vivo* (**Figure 4A-H**), suggesting this is
348 likely not the mechanism of decreased EAE susceptibility with Hbα-a1 knock-out in T-lymphocytes.
349 Understanding that $CD4^+$ T-lymphocytes interact with and potentiate inflammation from other immune cells
350 (i.e., B-lymphocytes) to promote EAE disease progression, we next queried levels of circulating antibodies in
351 the respective mouse models. Interestingly, HbKO EAE animals exhibited significantly lower levels of plasma
352 IgM and lambda immunoglobins compared to WT EAE animals, suggesting the loss of T-lymphocyte Hbα
353 caused a significant impact on B-lymphocyte antibody output **(Figure 4I-J)**. To explore this further, we
354 assessed receptors and ligands that are essential for the interaction between T-lymphocytes and B-
355 lymphocytes. While we did not find any differences in the number of cells expressing the costimulatory receptor
356 CD27 between HbKO and WT T-lymphocytes (**Supplementary Figure 4L**), we did observe significantly fewer
357 $CD4^+$ HbKO T-lymphocytes expressing CD40L (**Figure 4K**). Congruent with previous findings, no changes
358 were observed in $CD8^+$ T-lymphocytes (**Figure 4K**). Together, these data promote the hypothesis that the loss
359 of Hbα in T-lymphocytes leads to insufficient crosstalk with other immune cells, but additional work is warranted
360 to explore the full depth and repertoire of these deficient interactions.

361 **Discussion**

362 Hemoglobin is becoming increasingly recognized as a protein expressed in a variety of cell types
363 beyond erythrocytes, and has been shown to possess varying redox functions and regulatory mechanisms
364 throughout its diverse cellular potency (11, 12). We recently reported that Hbα is expressed in T-lymphocytes
365 and its expression is malleable to redox perturbations, suggesting a redox regulatory role (13). Herein, we
366 expand and refine our knowledge on Hbα expression at both the RNA and protein levels, explore its role in the
367 context of T-lymphocyte metabolism and activation, and define differences between $CD4^+$ and $CD8^+$ T-
368 lymphocyte subtypes. Altogether, our data suggest Hbα is an important T-lymphocyte redox-regulatory protein
369 that is crucial for maintaining mitochondrial bioenergetics and proper T-lymphocyte activation, particularly in
370 $CD4^+$ T-lymphocytes.

371 Previously, we demonstrated that Hbα-a1 mRNA expression was rapidly down regulated within 24
372 hours in total T-lymphocytes after activation, likely due to activation-promoted epigenetic remodeling (13).
373 Herein, we discovered that Hbα-a1 mRNA expression continues to decrease compared to naïve levels after 48
374 hours post activation in both $CD4^+$ and $CD8^+$ cells, but diverges depending on subtype at 72 hours.
375 Interestingly, Hbα protein expression revealed a differential pattern than the mRNA, with protein conversely
376 increasing after 24 hours post activation compared to naïve T-lymphocytes. These disparate levels suggest the
377 potential for a post-transcriptional regulatory mechanism between Hbα-a1 mRNA and Hbα protein. Moreover,
378 this robust increase in Hbα protein at 24 hours may be in response to the massive burst of ROS produced
379 during T-lymphocyte activation (23, 25, 28). While this burst of ROS is imperative for activation, uncontrolled
380 ROS can lead to cell death, and is therefore tightly controlled by a subsequent increase of antioxidants, such
381 as glutathione, Nrf2 activation, and as potentially described herein, Hbα (28, 29). In accordance with the mRNA
382 expression, protein expression decreased in both subtypes after 48 hours, but once again increased after 72
383 hours activation. This increase in Hbα protein at the later time point may represent the early stages of
384 polarization occurring in which certain subtypes of T-lymphocytes (i.e., memory T-lymphocytes, regulatory T-
385 lymphocytes, etc.) display significantly elevated levels of Hbα as we have previously shown (13). Overall, Hbα
386 seems to be intricately regulated at both the RNA and protein level in the major T-lymphocyte subtypes and
387 activation states. This dynamic regulatory pattern suggests Hbα is not a passive bystander in T-lymphocytes,
388 but instead plays an important and vital role that requires intricate and tight control.

389 While the functional role of non-canonical hemoglobin likely varies depending on cell type, it has been
390 hypothesized that its function may be linked to mitochondrial energetics (30-35). We too recently reported that
391 the loss of Hbα in T-lymphocytes significantly increased MitoSOX oxidation in a mouse model of psychological
392 trauma (13). To further explore this phenomenon here, we examined the mitochondrial phenotype of naïve and
393 activated T-lymphocyte subtypes. While there were no discernable differences between naïve WT and HbKO
394 T-lymphocytes, HbKO T-lymphocytes activated for 72 hours possessed greater MitoSOX oxidation and
395 significantly lower TMRE fluorescence, suggesting mitochondrial dysfunction. This dysfunction was more
396 prominent in $CD4^+$ T-lymphocytes, which concurrently showed a greater difference in mitochondrial
397 bioenergetics compared to their WT counterparts. Additionally, both $CD4^+$ and $CD8^+$ activated HbKO T-
398 lymphocytes showed a greater reliance on glucose as opposed to fatty acids/amino acids, further suggesting
399 the loss of Hbα may greatly impact mitochondrial metabolism. Interestingly, the observed increase in MitoSOX
400 oxidation, lower TMRE fluorescence, and decrease in overall OCR in HbKO $CD4^+$ T-lymphocytes is very
401 similar to T-lymphocytes that lack an important mitochondrial antioxidant, manganese superoxide dismutase
402 (MnSOD), further suggesting Hbα may play a similar role in modulating the mitochondrial redox environment of
403 activated T-lymphocytes (24).
404 In addition to disrupted mitochondrial bioenergetics, the loss of Hbα significantly altered the timing and
405 magnitude of cytokine production after activation. Both $CD4^+$ and $CD8^+$ HbKO T-lymphocytes produced higher
406 concentrations of specific cytokines such as IL-6 and IL-17A, but $CD4^+$ T-lymphocytes showed a more
407 pronounced phenotype with an apparent global loss of cytokine regulation, particularly 24 hours post-
408 activation. Additionally, $CD4^+$ HbKO T-lymphocytes produced higher concentrations of cytokines at 24 hours in
409 response to lower concentrations of CD3 stimuli, suggesting that the loss of Hbα lowers the threshold of
410 activation. The combination of greater mitochondrial dysfunction and increased production of proinflammatory
411 cytokines in HbKO $CD4^+$ T-lymphocytes may suggest that Hbα plays an important role in $CD4^+$ T-lymphocyte
412 activation and cytokine regulation. This pronounced phenomenon in helper T-lymphocytes may also help
413 explain the higher occurrence of autoimmune disorders and elevated inflammation in patients with
414 hemoglobinopathies (2-4, 36, 37).
415 Given this highly proinflammatory phenotype of HbKO T-lymphocytes *ex vivo,* we hypothesized that
416 loss of Hbα would accelerate autoimmune risk or progression. EAE induction with MOG_{35-55} was chosen due to

417 the important role of T-lymphocytes in developing the disease, as compared to MOG_{1-125} which is a primary B-
418 lymphocyte-mediated response (38, 39). To our surprise and contrary to our hypothesis, HbKO animals fared
419 better, showing delayed disease progression and less severe phenotypes. Intriguingly, both genotypes
420 exhibited similar levels of circulating cytokines, splenic T-lymphocyte percentages, $CD4^+$ T-lymphocyte
421 polarization subtypes, and antigen recall responses, indicating that decreased disease severity was likely not
422 due to decreased T-lymphocyte viability, differentiation, or cytokine production. HbKO animals did have less
423 $CD4^+$ T-lymphocytes present in the inguinal lymph nodes at 28 days compared to WT EAE lymph nodes, but
424 this difference was not apparent at the height of disease severity (i.e., 14 days). Moreover, HbKO T-
425 lymphocytes showed no differences in transwell migration towards either CXCL12 or RANTES (a cytokine
426 known to recruit T-lymphocytes to the CNS during EAE induction (40)), suggesting defects in T-lymphocyte
427 migration likely do not fully explain the decreased severity of EAE in HbKO animals. Therefore, in contrast to
428 the *ex vivo* findings, HbKO T-lymphocytes appear to possess many normal functions *in vivo*, at least in the
429 context of EAE.

430 However, while certain isolated T-lymphocyte functions appeared to be intact, their ability to interact
431 with other cell types essential for EAE development remained unclear. In EAE after $CD4^+$ T-lymphocytes are
432 activated and differentiated, T_H1 and T_H17 cells can extravasate into the spinal cord and interact with other
433 immune cells, like B-lymphocytes and microglia (41), which are partially responsible for damaging the myelin
434 sheath of the spinal cord and leading to paralysis symptoms. Strikingly, HbKO EAE animals exhibited a
435 significant reduction in plasma IgM and lambda immunoglobulins, two important immunoglobulins in EAE
436 induction (42). Taken together with previous data, this decrease in immunoglobulins suggested an impaired
437 interaction between T-lymphocytes and B-lymphocytes. To preliminarily test this hypothesis, T-lymphocytes
438 were assessed for CD40L and CD27, which are two extracellular markers known to interact with B-
439 lymphocytes (43-47). While no apparent differences were noted in percentage of cells expressing the CD27
440 receptor in HbKO T-lymphocytes, $CD4^+$ HbKO T-lymphocytes did exhibited fewer $CD40L^+$ cells after acute
441 activation (measured between its highest expression time point, 4-8 hours after activation (48)). Importantly,
442 the CD40-CD40L interaction has been shown to be critical in EAE development. It has been demonstrated that
443 blocking CD40 throughout the experimental duration significantly blunted EAE symptomology, suggesting the
444 receptor is necessary for demyelination (49). However, additional experiments are required to confirm if the

445 decrease in CD40L expression on HbKO T-lymphocytes is the definitive mechanism underlying the lessened
446 EAE severity.

447 One potential confounder of the work presented herein is the potential for hemoglobin compensation,
448 particularly of the alpha locus. Due to the importance of Hbα in adult hemoglobin tetramers, many mammalian
449 species (including humans and mice) have evolved two identical copies of the gene: Hbα-a1 and Hbα-a2.
450 Therefore, since our genetic knock-out model was specific for Hbα-a1, it remains unclear if/how Hbα-a2 plays
451 a role (or compensation) in T-lymphocytes. Anecdotally, we are still able to detect Hbα protein in HbKO T-
452 lymphocytes (data not shown), which suggests Hbα-a2 must be expressed at some level in these cells.
453 However, the loss of Hbα-a1 **(**even with potential expression of Hbα-a2) was effective enough to cause a
454 significant phenotype in T-lymphocytes, so compensation from this locus is not fully complete. Additionally, we
455 previously reported detection of beta hemoglobin mRNA in T-lymphocytes as well (13), but found it had very
456 different expression patterns compared to the alpha subtypes. Many hemoglobinopathies are due to mutations
457 or loss of beta hemoglobin loci, but its role in T-lymphocytes remains unknown to date. Last, while we used
458 CD4-cre to induce the recombination of Hbα-a1 in T-lymphocytes, this model initiates knock-out during T-
459 lymphocyte development in this thymus. While we did not observe any baseline changes in total T-lymphocyte
460 numbers or distributions of major subtypes in HbKO animals, it does raise the possibility that the loss of Hbα-
461 a1 during development caused the observed phenotype. Using our Hbα-a1 animals with an inducible T-
462 lymphocyte-driven cre-recombinase in the future will address this potential confounder.

463 In summary, our data suggest that Hbα is an intricately controlled redox protein temporally expressed in
464 T-lymphocytes subtypes. The loss of Hbα in T-lymphocytes leads to mitochondrial dysfunction, decreased
465 activation potential, and heightened production of inflammatory cytokines, potentially shedding light on the
466 current unknown connection between hemoglobinopathies and autoimmune disorders. Modern molecular tools
467 have allowed us to define the critical nature of Hbα in T-lymphocytes, where it was not even reported to exist,
468 and fully elucidating the regulatory mechanisms and functional role(s) of Hbα within T-lymphocytes will expand
469 our knowledge of T-lymphocyte activation, polarization, and mitochondrial regulation. Additionally, our findings
470 may provide a missing link between autoimmune etiologies in patients with hemoglobinopathies and could
471 pave the way for immune cell-targeted treatments for these patients, rather than solely focusing on
472 erythrocytes.

473 **Acknowledgements**

474 **Funding sources**

475 This work was supported by the National Institutes of Health (NIH) R01HL158521 (AJC) and T32GM135115
476 (ECR). We thank Dr. Brant Isakson for his contribution of the Hbα-a1 floxed mouse model used in this work.
477 We thank Texas A&M University's College of Medicine Flow Cytometry and Cell Sorting Facility for the use of
478 their Seahorse Bioanalyzer, as well as Texas A&M University's Rodent Preclinical Phenotyping Core for the
479 use of the Protein Simple Jess Automated Western Blot and Vetscan HM5 Hematology Analyzer.

480

481 **Author contributions**

482 ECR and AJC designed research studies. All authors conducted experiments, acquired data, and/or performed
483 analyses. ECR and AJC wrote the manuscript, while all authors approved the final version of the manuscript.
484 AJC provided funding and experimental oversight.

485

486 **Abbreviations:** Hbα-a1, hemoglobin alpha-a1 mRNA; Hbα, hemoglobin alpha protein; O_2, oxygen; NO, nitric
487 oxide; HbKO, T-lymphocyte specific hemoglobin alpha-a1 knock out mice; ROS, reactive oxygen species;
488 EAE, experimental autoimmune encephalomyelitis;

489 **Figure Legends**

490 **Figure 1: Activation state of T-lymphocytes determines intracellular Hbα levels and impact on**
491 **mitochondria. A-D**: Hbα-a1 mRNA (N=7) and Hbα protein expression (N=7) over 24, 48, 72-hour time points
492 after activation of $CD4^+$ (**A-B**) and $CD8^+$ (**C-D**) T-lymphocytes compared to naive T-lymphocytes (N=6). **E-H**:
493 Splenic $CD4^+$ and $CD8^+$ T-lymphocytes were isolated and activated for 72 hours, then assessed by flow
494 cytometric analysis of MitoSOX (**E-F**) and TMRE MFI (**G-H**). **I-L**: Splenic $CD4^+$ and $CD8^+$ T-lymphocytes were
495 isolated and activated for 72 hours, then assessed using Seahorse mitochondrial stress test (N=5). R+A =
496 rotenone + antimycin A. **M-T**: Splenic T-lymphocytes were activated for 72 hours, then puromycin MFI was
497 measured via SCENITH protocol in $CD4^+$ and $CD8^+$ T-lymphocytes to obtain calculations graphed (reported in
498 percentage). Statistics measured by a one-way ANOVA with Dunnett's multiple comparisons test, unpaired
499 Student's t-test, or two-way ANOVA with Šídák's multiple comparisons test where appropriate.

500

501 **Figure 2: Activated HbKO T-lymphocytes exhibit an accelerated and enhanced proinflammatory**
502 **phenotype. A-H**: Extracellular cytokine protein measured from $CD4^+$ (**A-D**) and $CD8^+$ (**E-H**) T-lymphocytes at
503 24, 48, 72 hours post-activation (pg/mL per 10^6 cells) (N=5). **I-P**: Extracellular cytokine protein measured from
504 $CD4^+$ (**I-L**) and $CD8^+$ (**M-P**) T-lymphocytes treated for 24 hours with anti-CD28 and varying concentrations of
505 anti-CD3 (N=3). Statistics measured using unpaired Student's t-test, mixed-effects analysis, or two-way
506 ANOVA with Šídák's multiple comparisons test where appropriate.

507

508 **Figure 3: HbKO EAE animals exhibit better disease phenotypes but similar inflammatory profiles as WT**
509 **EAE animals. A**: Schematic of 28-day EAE experimental design. **B-C**: EAE severity scores (0-5) and weights
510 (g) over 28-day incubation period (WT N=14, HbKO N=10). **D-G**: Protein concentration (pg/mL) of cytokines in
511 plasma. **H-K:** Percentage of $CD4^+$ and $CD8^+$ present in the spleen and inguinal lymph nodes at day 28. **L-O**:
512 Percentage of splenic $CD4^+$ polarized T-lymphocytes. **P-S**: Splenocytes restimulated with 10 µg/mL MOG_{35-55}
513 for 72 hours, then assessed for extracellular cytokine protein concentration (pg/mL per 10^6 cells). Statistics
514 measured by two-way ANOVA with Šídák's multiple comparisons test or Student's t-test where appropriate.

515

516 **Figure 4: Loss of Hbα impairs T-lymphocyte intercellular communication. A-H**: Splenic T-lymphocytes
517 were isolated and activated with a 1:1 ratio of Dynabeads for 72 hours, replated into transwell inserts over
518 control, RANTES, or CXCL12 media for 4 hours, then total cell counts (**A-D**) and ratio of cells migrated over
519 control well migration (**E-H**) were assessed by flow cytometry. **I-J**: Relative IgM and lambda immunoglobulin
520 concentrations in plasma from 14-day EAE animals (AU: arbitrary units). **K-L**: Splenic T-lymphocytes were
521 isolated and assessed at 4-hour activated (**L**) and 24-hour activated (**K**) for receptor expression by flow
522 cytometry. Statistics measured using Student's t-test. Statistics (only significant shown) were measured by two-
523 way ANOVA with Šídák's multiple comparisons test or student's t-test where appropriate.
524
525 **Supplementary Figure 1: Generation of T-lymphocyte specific hemoglobin alpha a1 knock-out animals.**
526 **A**: Schematic of T-lymphocyte specific Hbα-a1 mouse knock out (HbKO) generation. **B**: Results of tail, liver,
527 and isolated pan T-lymphocytes genotyped for Hbα-a1 excision (WT: 1088bp, excised: ~500bp). **C-F**:
528 Complete blood count results of hemoglobin (**C**), white blood cells (**D**), red blood cells (**E**), and lymphocytes (**F**)
529 from whole blood samples from WT and HbKO animals. **G-H**: Splenic percentages of $CD4^+$ (**G**) and $CD8^+$ (**H**)
530 T-lymphocytes in WT and HbKO animals. **I-J**: Live cell counts of $CD4^+$ (**I**) and $CD8^+$ T-lymphocytes (**J**) isolated
531 from whole spleens. **K-L**: Growth curves of activated isolated splenic $CD4^+$ (**K**) and $CD8^+$ (**L**) T-lymphocytes
532 over 24, 48, 72 hours (N=6). **M-R**: Naïve splenic $CD4^+$ and $CD8^+$ T-lymphocytes were isolated and measured
533 for MitoSOX (**M-N**), DHE (**O-P**), and DAF-FM (**Q-R**) (mean fluorescence intensity). Statistics (not significant,
534 not shown) were measured using Student's t-test or two-way ANOVA.
535
536 **Supplementary Figure 2: Additional cytokines measured in T-lymphocyte time course activation.**
537 Extracellular cytokine protein concentration from activated $CD4^+$ (**A-D**) and $CD8^+$ T-lymphocytes (**E-H**) from WT
538 and HbKO animals (N=5). Statistics measured using two-way ANOVA.
539
540 **Supplementary Figure 3: Fourteen day EAE procedure. A**: Schematic of 14-day EAE experimental design.
541 **B-C**: EAE severity scores (0-5) and mouse weights (g) over 14-day incubation period (WT N=30, HbKO N=25).
542 **D-G**: Protein concentration (pg/mL) of cytokines in plasma. **H-K**: Percentage of $CD4^+$ and $CD8^+$ present in the
543 spleen and lymph nodes at day 14. **L-O**: Percentage of splenic CD4+ polarized T-lymphocytes. **P-S**:

544 Splenocytes restimulated with 10 μg/mL MOG_{35-55} for 72 hours, then assessed for extracellular cytokine protein
545 concentration (pg/mL per 10^6 cells). Statistics measured by two-way ANOVA with Šídák's multiple comparisons
546 test or Student's t-test where appropriate.
547
548 **Supplementary Figure 4: Splenic and spinal cord immune cell percentages do not change between WT**
549 **and HbKO EAE animals. A-D**: Percentage of inguinal lymph node CD4+ polarized T-lymphocytes. **E-H**:
550 Immune cell populations of B-lymphocytes (**E**), dendritic cells (**F**), granulocytes (**G**) and monocytes (**H**) were
551 assessed by flow cytometry. **I-J**: MitoSOX MFI of $CD4^+$ (**I**) and $CD8^+$ (**J**) splenic T-lymphocytes. **K**: Percentage
552 of $CD45^+$ cells present in the spinal cord. **L**: Live cell count of splenocytes after 72-hour restimulation with 10
553 μg/mL MOG_{35-55}. Statistics (not significant, not shown) were measured using Student's t-test.

554 **References**

555 1. T. N. Williams, D. J. Weatherall, World distribution, population genetics, and health burden of the
556 hemoglobinopathies. *Cold Spring Harb Perspect Med* **2**, a011692 (2012).

557 2. M. Hughes, Q. Akram, D. C. Rees, A. K. Jones, Haemoglobinopathies and the rheumatologist.
558 *Rheumatology (Oxford)* **55**, 2109-2118 (2016).

559 3. M. Tang, E. Nur, C. Van Tuijn, B. Biemond, Higher Prevalence of Autoimmune Diseases in Patients with
560 Sickle Cell Disease. *Blood* **138** (2021).

561 4. G. El Hasbani, K. M. Musallam, I. Uthman, M. D. Cappellini, A. T. Taher, Thalassemia and autoimmune
562 diseases: Absence of evidence or evidence of absence? *Blood Rev* **52**, 100874 (2022).

563 5. K. R. Atkuri, L. A. Herzenberg, A. K. Niemi, T. Cowan, Importance of culturing primary lymphocytes at
564 physiological oxygen levels. *Proc Natl Acad Sci U S A* **104**, 4547-4552 (2007).

565 6. Y. Ohyagi, T. Yamada, I. Goto, Hemoglobin as a novel protein developmentally regulated in neurons.
566 *Brain Res* **635**, 323-327 (1994).

567 7. F. Richter, B. H. Meurers, C. Zhu, V. P. Medvedeva, M. F. Chesselet, Neurons express hemoglobin
568 alpha- and beta-chains in rat and human brains. *J Comp Neurol* **515**, 538-547 (2009).

569 8. D. W. Schelshorn *et al.*, Expression of hemoglobin in rodent neurons. *J Cereb Blood Flow Metab* **29**,
570 585-595 (2009).

571 9. L. Liu, M. Zeng, J. S. Stamler, Hemoglobin induction in mouse macrophages. *Proc Natl Acad Sci U S A*
572 **96**, 6643-6647 (1999).

573 10. H. Nishi *et al.*, Hemoglobin is expressed by mesangial cells and reduces oxidant stress. *J Am Soc*
574 *Nephrol* **19**, 1500-1508 (2008).

575 11. D. Saha *et al.*, Hemoglobin expression in nonerythroid cells: novel or ubiquitous? *Int J Inflam* **2014**,
576 803237 (2014).

577 12. E. C. Reed, J. D. Kim, A. J. Case, Non-canonical hemoglobin: An updated review on its ubiquitous
578 expression. *Redox Biol* **82**, 103602 (2025).

579 13. E. C. Reed *et al.*, Hemoglobin alpha is a redox-sensitive mitochondrial-related protein in T-lymphocytes.
580 *Free Radic Biol Med* **227**, 1-11 (2024).

581 14. T. C. S. Keller *et al.*, Endothelial alpha globin is a nitrite reductase. *Nat Commun* **13**, 6405 (2022).

582 15. P. P. Lee *et al.*, A critical role for Dnmt1 and DNA methylation in T cell development, function, and
583 survival. *Immunity* **15**, 763-774 (2001).

584 16. N. Percie du Sert *et al.*, The ARRIVE guidelines 2.0: updated guidelines for reporting animal research. *J*
585 *Physiol* **598**, 3793-3801 (2020).

586 17. T. H. Lauten *et al.*, Beta Adrenergic Signaling as a Therapeutic Target for Autoimmunity. *bioRxiv* (2025).

587 18. A. J. Case, C. T. Roessner, J. Tian, M. C. Zimmerman, Mitochondrial Superoxide Signaling Contributes
588 to Norepinephrine-Mediated T-Lymphocyte Cytokine Profiles. *PLoS One* **11**, e0164609 (2016).

589 19. T. H. Lauten *et al.*, T H 17/Treg lymphocyte balance is regulated by beta adrenergic and cAMP
590 signaling. *Brain Behav Immun* **123**, 1061-1070 (2024).

591 20. S. K. Elkhatib, C. M. Moshfegh, G. F. Watson, A. J. Case, T-lymphocyte tyrosine hydroxylase regulates
592 T H 17 T-lymphocytes during repeated social defeat stress. *Brain Behav Immun* **104**, 18-28 (2022).

593 21. C. M. Moshfegh *et al.*, S100a9 Protects Against the Effects of Repeated Social Defeat Stress.
594 *Biological Psychiatry Global Open Science* (2022).

595 22. R. J. Argüello *et al.*, SCENITH: A Flow Cytometry-Based Method to Functionally Profile Energy
596 Metabolism with Single-Cell Resolution. *Cell Metab* **32**, 1063-1075.e1067 (2020).

597 23. A. J. Case *et al.*, Elevated mitochondrial superoxide disrupts normal T cell development, impairing
598 adaptive immune responses to an influenza challenge. *Free Radic Biol Med* **50**, 448-458 (2011).

599 24. C. M. Moshfegh *et al.*, Mitochondrial superoxide disrupts the metabolic and epigenetic landscape of
600 CD4(+) and CD8(+) T-lymphocytes. *Redox biology*, 101141 (2019).

601 25. L. A. Sena *et al.*, Mitochondria are required for antigen-specific T cell activation through reactive oxygen
602 species signaling. *Immunity* **38**, 225-236 (2013).

603 26. E. L. Pearce, M. C. Poffenberger, C. H. Chang, R. G. Jones, Fueling immunity: insights into metabolism
604 and lymphocyte function. *Science* **342**, 1242454 (2013).

605 27. M. El-behi, A. Rostami, B. Ciric, Current views on the roles of Th1 and Th17 cells in experimental
606 autoimmune encephalomyelitis. *J Neuroimmune Pharmacol* **5**, 189-197 (2010).

607 28. E. L. Yarosz, C. H. Chang, The Role of Reactive Oxygen Species in Regulating T Cell-mediated
608 Immunity and Disease. *Immune Netw* **18**, e14 (2018).

609 29. K. Pilipow *et al.*, Antioxidant metabolism regulates CD8+ T memory stem cell formation and antitumor
610 immunity. *JCI Insight* **3** (2018).

611 30. M. Biagioli *et al.*, Unexpected expression of alpha- and beta-globin in mesencephalic dopaminergic
612 neurons and glial cells. *Proc Natl Acad Sci U S A* **106**, 15454-15459 (2009).

613 31. I. Ferrer *et al.*, Neuronal hemoglobin is reduced in Alzheimer's disease, argyrophilic grain disease,
614 Parkinson's disease, and dementia with Lewy bodies. *J Alzheimers Dis* **23**, 537-550 (2011).

615 32. L. Broadwater *et al.*, Analysis of the mitochondrial proteome in multiple sclerosis cortex. *Biochim*
616 *Biophys Acta* **1812**, 630-641 (2011).

617 33. F. Shephard, O. Greville-Heygate, O. Marsh, S. Anderson, L. Chakrabarti, A mitochondrial location for
618 haemoglobins--dynamic distribution in ageing and Parkinson's disease. *Mitochondrion* **14**, 64-72
619 (2014).

620 34. W. Yang, X. Li, S. Yu, Neuronal hemoglobin in mitochondria is reduced by forming a complex with α-
621 synuclein in aging monkey brains. *Oncotarget* **7**, 7441-7454 (2016).

622 35. A. Brunyanszki *et al.*, Upregulation and Mitochondrial Sequestration of Hemoglobin Occur in Circulating
623 Leukocytes during Critical Illness, Conferring a Cytoprotective Phenotype. *Mol Med* **21**, 666-675 (2015).

624 36. I. C. P. Gomes *et al.*, Levels of inflammatory markers are differentially expressed in sickle cell anemia
625 and sickle cell trait. *EJHaem* **4**, 705-709 (2023).

626 37. E. Balandya, T. Reynolds, S. Obaro, J. Makani, Alteration of lymphocyte phenotype and function in
627 sickle cell anemia: Implications for vaccine responses. *Am J Hematol* **91**, 938-946 (2016).

628 38. H. H. Hofstetter *et al.*, The cytokine signature of MOG-specific CD4 cells in the EAE of C57BL/6 mice. *J*
629 *Neuroimmunol* **170**, 105-114 (2005).

630 39. J. M. Fletcher, S. J. Lalor, C. M. Sweeney, N. Tubridy, K. H. Mills, T cells in multiple sclerosis and
631 experimental autoimmune encephalomyelitis. *Clin Exp Immunol* **162**, 1-11 (2010).

632 40. A. R. Glabinski, V. K. Tuohy, R. M. Ransohoff, Expression of chemokines RANTES, MIP-1alpha and
633 GRO-alpha correlates with inflammation in acute experimental autoimmune encephalomyelitis.
634 *Neuroimmunomodulation* **5**, 166-171 (1998).

635 41. D. J. Burrows *et al.*, Animal models of multiple sclerosis: From rodents to zebrafish. *Mult Scler* **25**, 306-
636 324 (2019).

637 42. K. G. Haanstra *et al.*, Induction of experimental autoimmune encephalomyelitis with recombinant
638 human myelin oligodendrocyte glycoprotein in incomplete Freund's adjuvant in three non-human
639 primate species. *J Neuroimmune Pharmacol* **8**, 1251-1264 (2013).

640 43. A. Ara, K. A. Ahmed, J. Xiang, Multiple effects of CD40-CD40L axis in immunity against infection and
641 cancer. *Immunotargets Ther* **7**, 55-61 (2018).

642 44. V. Pucino, D. H. Gardner, B. A. Fisher, Rationale for CD40 pathway blockade in autoimmune rheumatic
643 disorders. *Lancet Rheumatol* **2**, e292-e301 (2020).

644 45. J. Hendriks *et al.*, CD27 is required for generation and long-term maintenance of T cell immunity. *Nat*
645 *Immunol* **1**, 433-440 (2000).

646 46. A. N. Vallejo, C. M. Weyand, J. J. Goronzy, T-cell senescence: a culprit of immune abnormalities in
647 chronic inflammation and persistent infection. *Trends Mol Med* **10**, 119-124 (2004).

648 47. Y. Lu *et al.*, T-cell senescence: A crucial player in autoimmune diseases. *Clin Immunol* **248**, 109202
649 (2023).

650 48. M. Roy, T. Waldschmidt, A. Aruffo, J. A. Ledbetter, R. J. Noelle, The regulation of the expression of
651 gp39, the CD40 ligand, on normal and cloned CD4+ T cells. *J Immunol* **151**, 2497-2510 (1993).

652 49. L. Boon *et al.*, Prevention of experimental autoimmune encephalomyelitis in the common marmoset
653 (Callithrix jacchus) using a chimeric antagonist monoclonal antibody against human CD40 is associated
654 with altered B cell responses. *J Immunol* **167**, 2942-2949 (2001).

655 50. N. Brown *et al.*, Neuronal Hemoglobin Expression and Its Relevance to Multiple Sclerosis
656 Neuropathology. *J Mol Neurosci* **59**, 1-17 (2016).

657

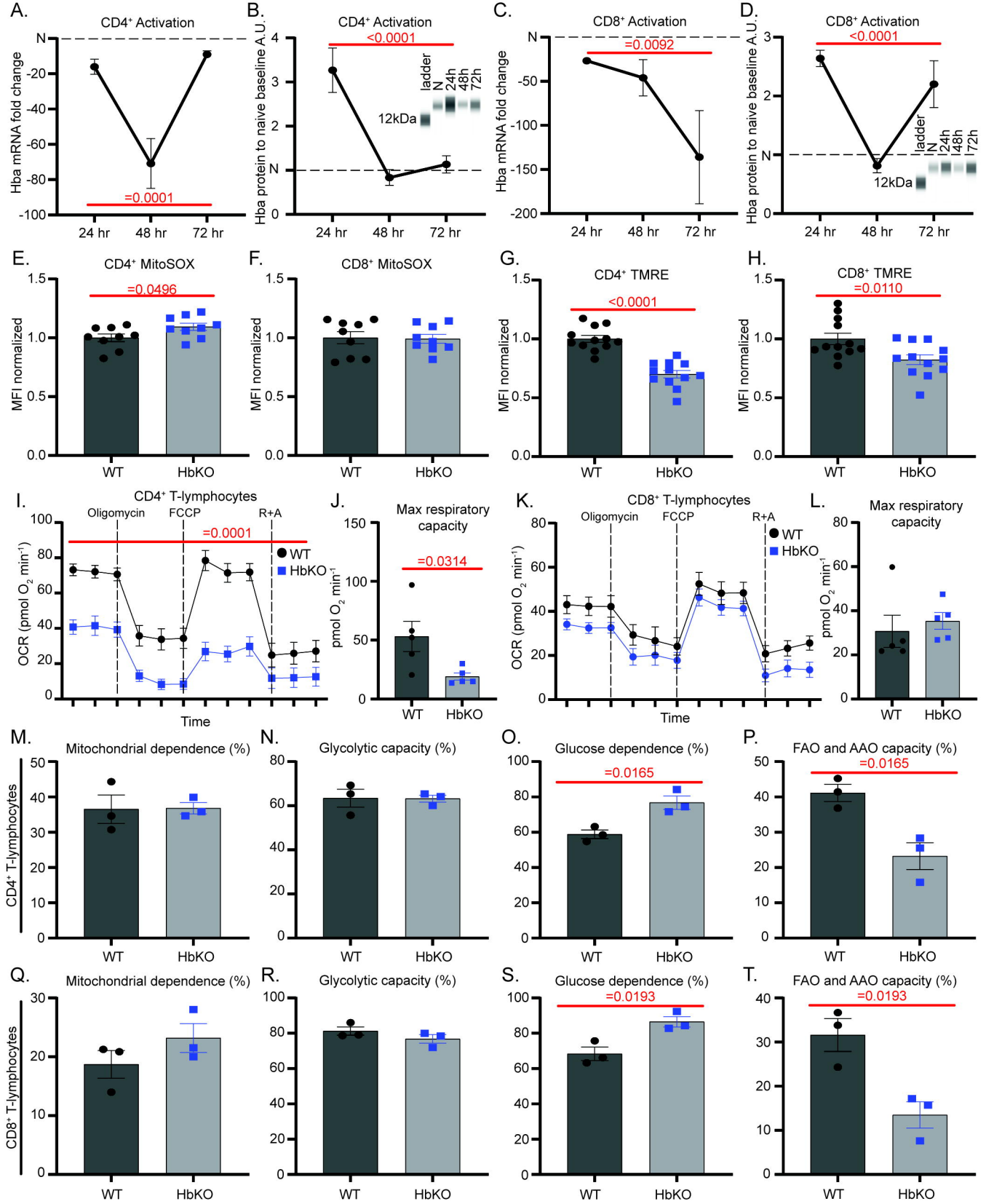
A.
CD4⁺ Activation
Hba mRNA fold change
N
-20
-40
-60
-80
-100
=0.0001
24 hr
48 hr
72 hr
B.
CD4⁺ Activation
Hba protein to naive baseline A.U.
<0.0001
ladder
N
24h
48h
72h
12kDa
C.
CD8⁺ Activation
Hba mRNA fold change
=0.0092
D.
CD8⁺ Activation
Hba protein to naive baseline A.U.
<0.0001
E.
CD4⁺ MitoSOX
MFI normalized
=0.0496
WT
HbKO
F.
CD8⁺ MitoSOX
G.
CD4⁺ TMRE
<0.0001
H.
CD8⁺ TMRE
=0.0110
I.
CD4⁺ T-lymphocytes
Oligomycin
FCCP
R+A
=0.0001
OCR (pmol O2 min-1)
Time
J.
Max respiratory capacity
pmol O2 min-1
=0.0314
K.
CD8⁺ T-lymphocytes
L.
M.
Mitochondrial dependence (%)
CD4⁺ T-lymphocytes
N.
Glycolytic capacity (%)
O.
Glucose dependence (%)
=0.0165
P.
FAO and AAO capacity (%)
=0.0165
Q.
Mitochondrial dependence (%)
CD8⁺ T-lymphocytes
R.
Glycolytic capacity (%)
S.
Glucose dependence (%)
=0.0193
T.
FAO and AAO capacity (%)
=0.0193

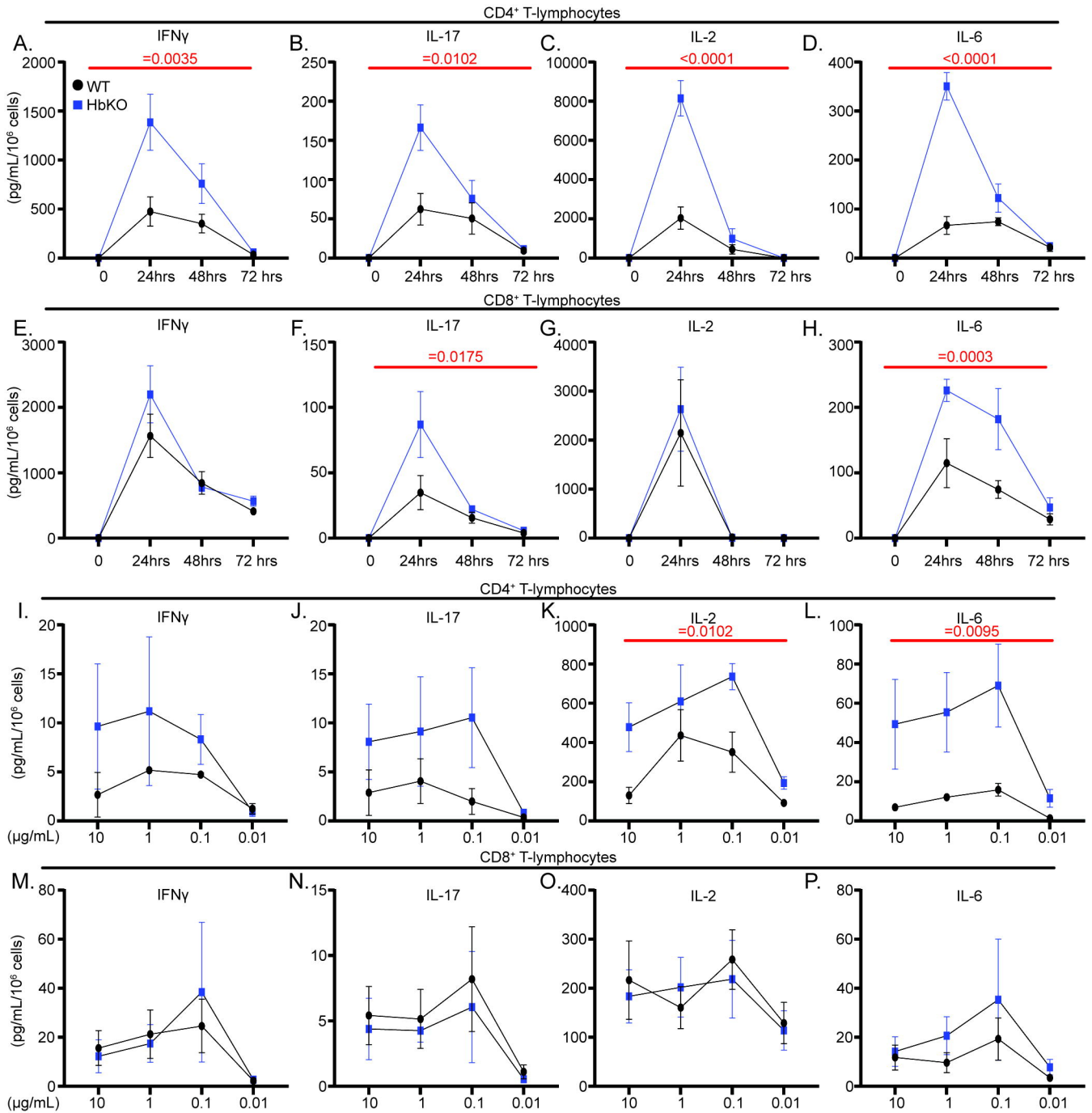
CD4+ T-lymphocytes
A.
IFNγ
=0.0035
WT
HbKO
(pg/mL/10^6 cells)
B.
IL-17
=0.0102
C.
IL-2
<0.0001
D.
IL-6
<0.0001
0
24hrs
48hrs
72 hrs
CD8+ T-lymphocytes
E.
IFNγ
F.
IL-17
=0.0175
G.
IL-2
H.
IL-6
=0.0003
CD4+ T-lymphocytes
I.
IFNγ
J.
IL-17
K.
IL-2
=0.0102
L.
IL-6
=0.0095
(μg/mL)
10
1
0.1
0.01
CD8+ T-lymphocytes
M.
IFNγ
N.
IL-17
O.
IL-2
P.
IL-6

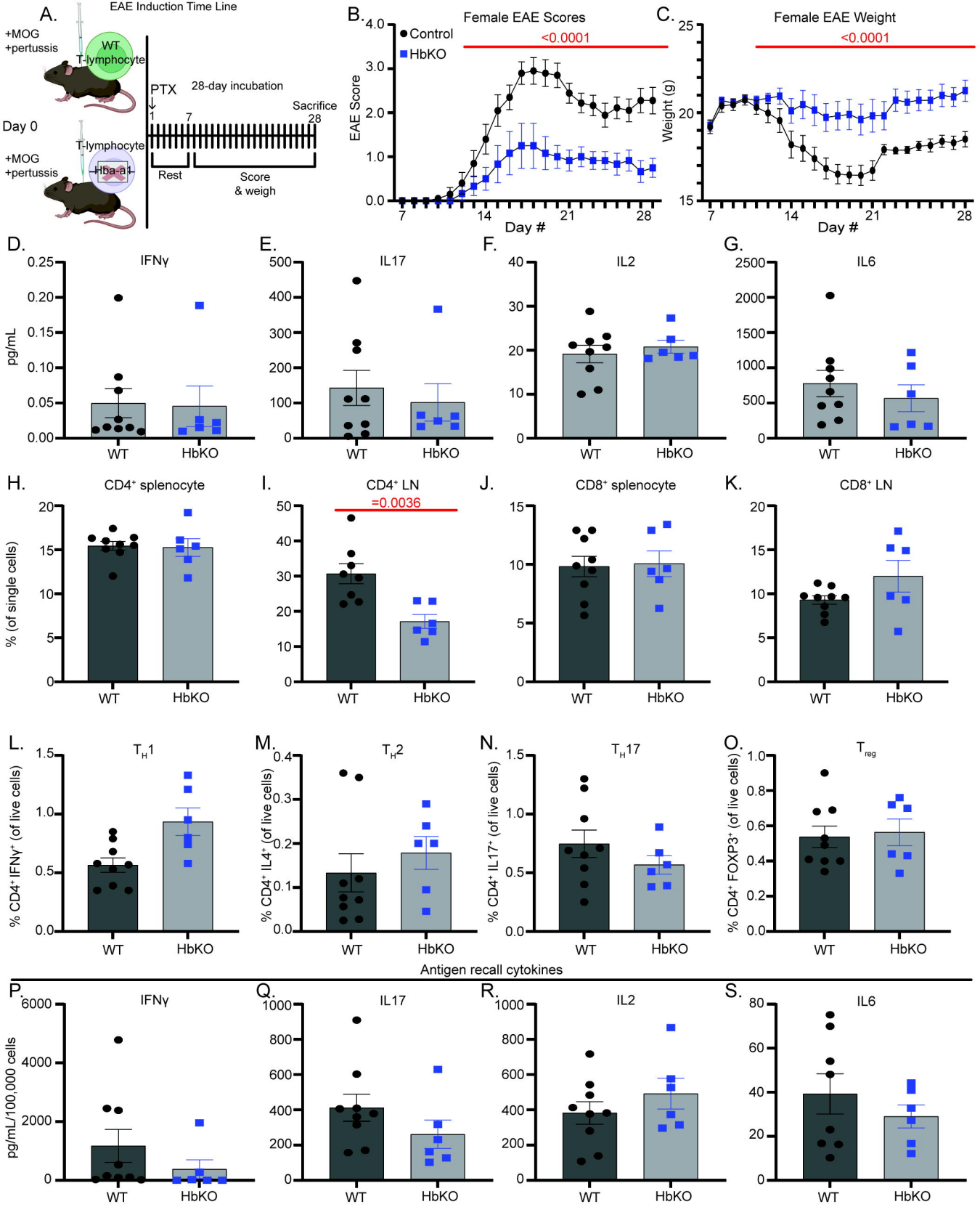
A.
EAE Induction Time Line
+MOG
+pertussis
WT
T-lymphocyte
Day 0
T-lymphocyte
+MOG
+pertussis
Hba-a1-
PTX
28-day incubation
Sacrifice
1
7
28
Rest
Score
& weigh
B.
Female EAE Scores
Control
HbKO
<0.0001
EAE Score
Day #
C.
Female EAE Weight
<0.0001
Weight (g)
Day #
D.
IFNγ
pg/mL
E.
IL17
F.
IL2
G.
IL6
H.
CD4⁺ splenocyte
% (of single cells)
I.
CD4⁺ LN
=0.0036
J.
CD8⁺ splenocyte
K.
CD8⁺ LN
L.
T_H1
% CD4⁺ IFNγ⁺ (of live cells)
M.
T_H2
% CD4⁺ IL4⁺ (of live cells)
N.
T_H17
% CD4⁺ IL17⁺ (of live cells)
O.
T_reg
% CD4⁺ FOXP3⁺ (of live cells)
WT
HbKO
Antigen recall cytokines
P.
IFNγ
pg/mL/100,000 cells
Q.
IL17
R.
IL2
S.
IL6

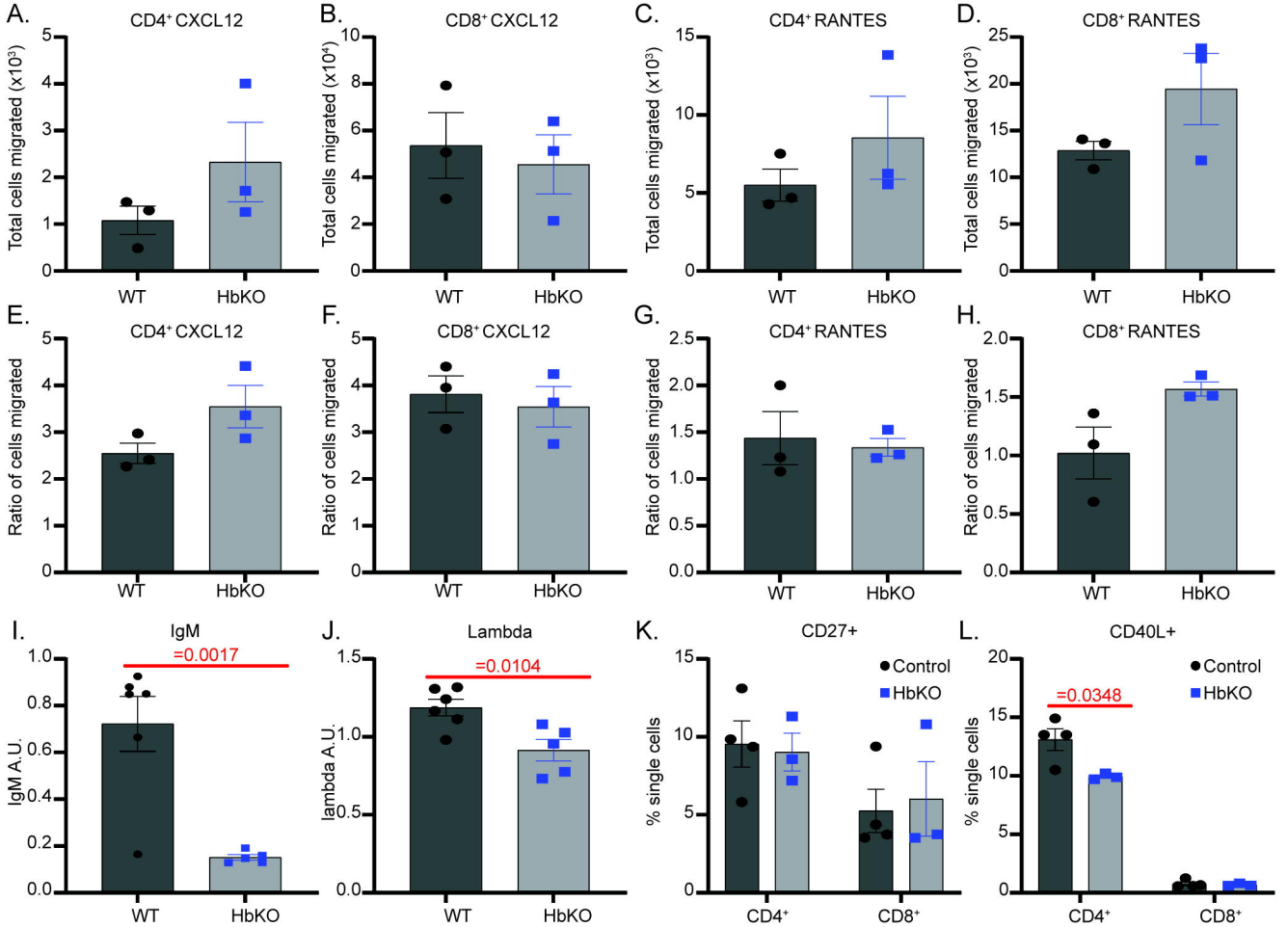
A.
CD4+ CXCL12
Total cells migrated (x10³)
WT
HbKO
B.
CD8+ CXCL12
Total cells migrated (x10⁴)
C.
CD4+ RANTES
Total cells migrated (x10³)
D.
CD8+ RANTES
Total cells migrated (x10³)
E.
CD4+ CXCL12
Ratio of cells migrated
F.
CD8+ CXCL12
G.
CD4+ RANTES
H.
CD8+ RANTES
I.
IgM
=0.0017
IgM A.U.
J.
Lambda
=0.0104
lambda A.U.
K.
CD27+
Control
HbKO
% single cells
CD4+
CD8+
L.
CD40L+
=0.0348